

Overview of the Design, Fabrication and Performance Requirements of μ -Spec, An Integrated Submillimeter Spectrometer

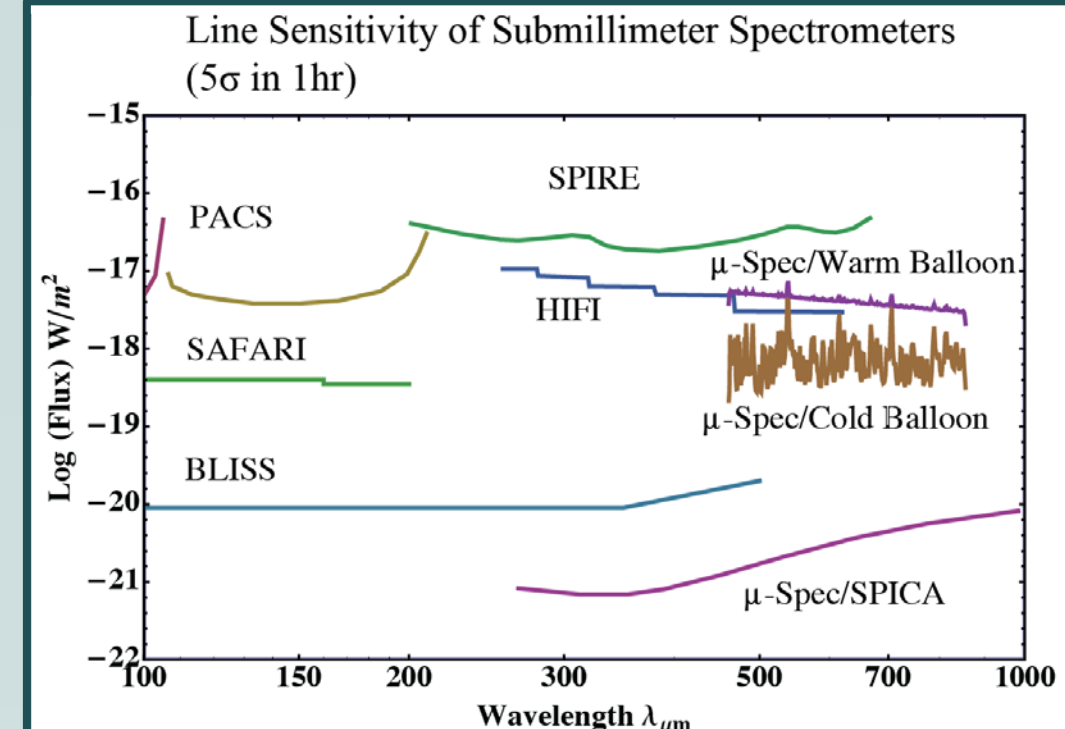
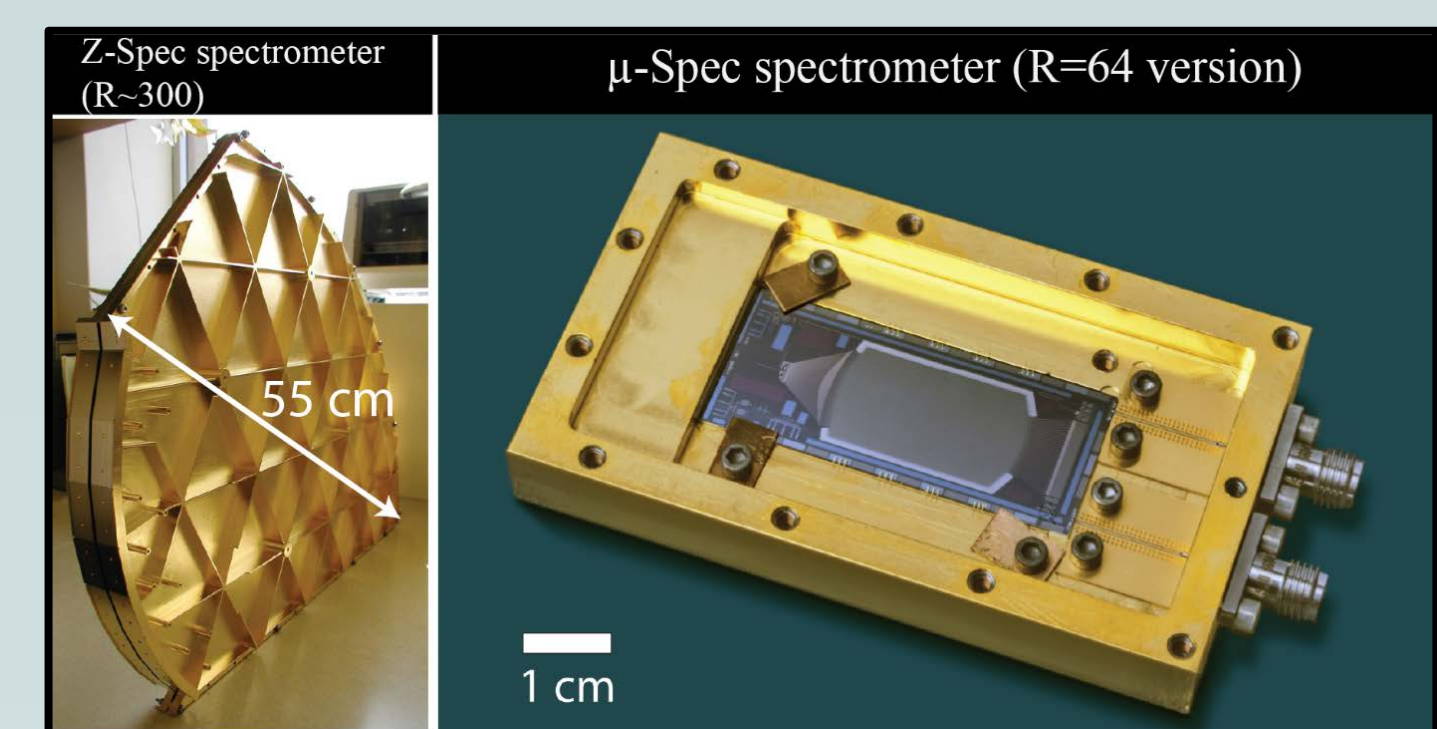


Emily M. Barrentine, Omid Noroozian, Ari D. Brown, Giuseppe Cataldo, Negar Ehsan, Wen-Ting Hsieh, Thomas R. Stevenson, Kongpop U-Yen, Edward J. Wollack, S. Harvey Moseley
NASA Goddard Space Flight Center, Greenbelt, MD 20771 USA

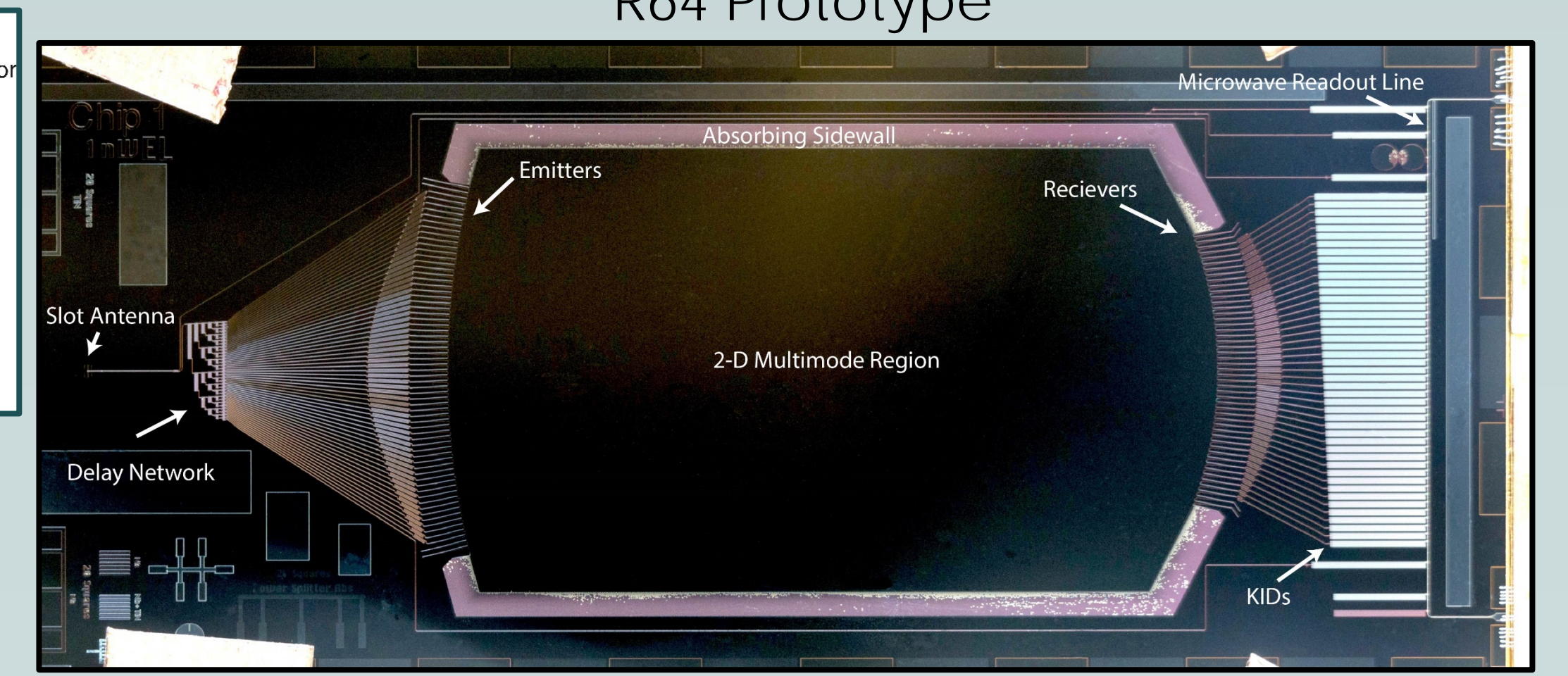
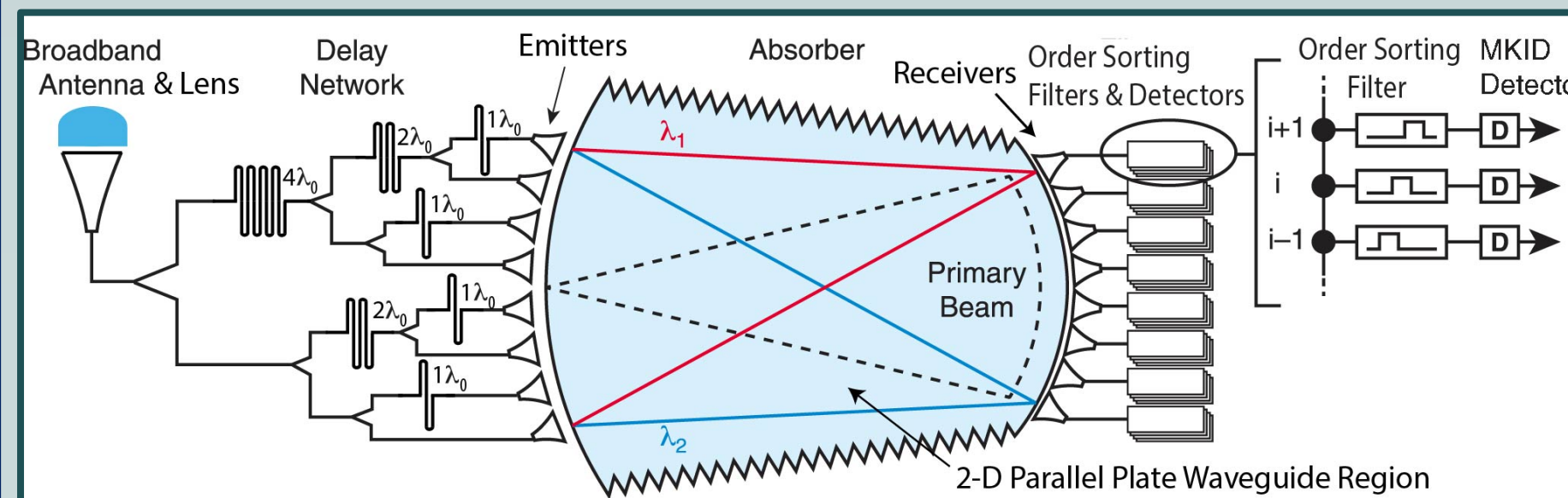
Abstract: μ -Spec is a compact submillimeter (350-700 GHz) spectrometer which uses low loss superconducting niobium microstrip transmission lines and a single-crystal silicon dielectric to integrate all of the components of a grating-analog spectrometer onto a single chip. Here we present details of the fabrication and design of a prototype μ -Spec spectrometer with resolution, $R=64$. We discuss some of the design concerns (such as loss, stray-light, cross-talk, and fabrication tolerances) for each of the spectrometer components and their integration into the instrument as a whole. We have demonstrated this prototype spectrometer with design resolution of $R=64$. Given the optical performance of this prototype, we will also discuss the extension of this design to higher resolutions suitable for balloon-flight.

Instrument Science Goals:

- The main science goals are to trace the evolution of physical conditions of the interstellar medium in both normal and star-forming galaxies across cosmic time.
- A spectrometer operating from 420 – 800 μ m can observe fine structure lines in star forming galaxies from $z = 2 - 8$.
- Arrays of hundreds of spectrometers would transform the capability of a space mission, such as the Far-Infrared Surveyor, being considered in the next Decadal Survey (see bottom-right).
- The current state-of-the-art is unable to meet these instrument requirements, due to size, weight and power constraints (see bottom-left and sensitivity limitations).



μ -Spec: An Integrated Sub-mm Grating-Analog Spectrometer

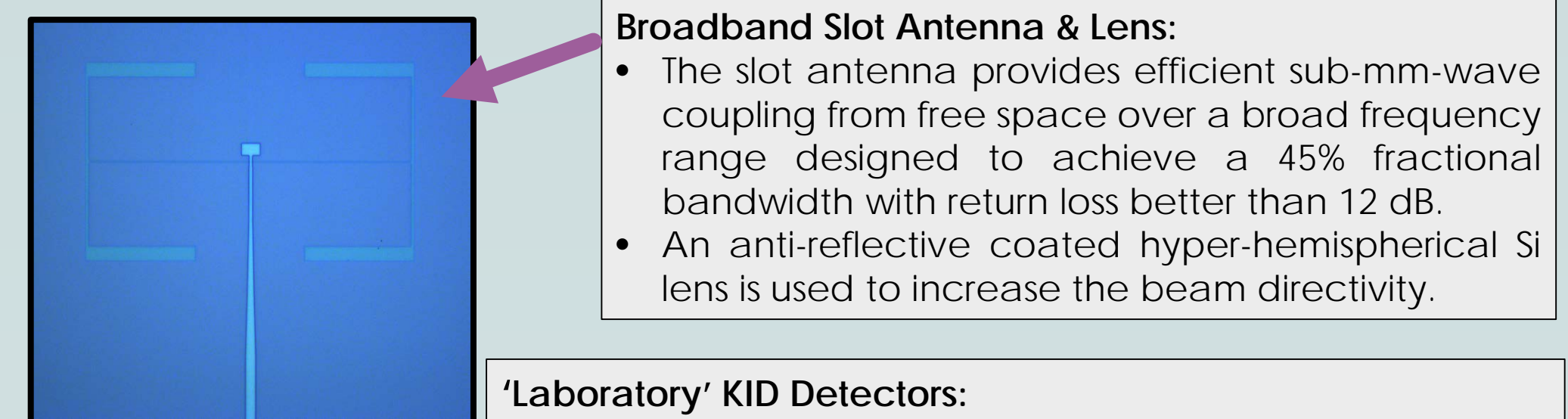


Advantages Due to The Diffraction-Analog Design:

- Intrinsically high efficiency.
- Insensitivity to lithographic errors and other fabrication variations.
- Uniform Nyquist spectral sampling and repeatability from device to device.
- Good spectral purity. The spectral function of the instrument is $(\sin(x)/x)^2$, the Fourier transform of the uniformly illuminated synthetic grating.

R=64 Instrument Components:

Many of the components of the μ -Spec instrument are required for any integrated instrument of this kind: such as highly efficient but controlled optical coupling to the sky, low loss superconducting transmission lines, KID detectors and microwave readout. The delay network, multimode region, focal plane and emitter and receivers are unique components necessary for the diffraction-analog spectrometer design.



Broadband Slot Antenna & Lens:

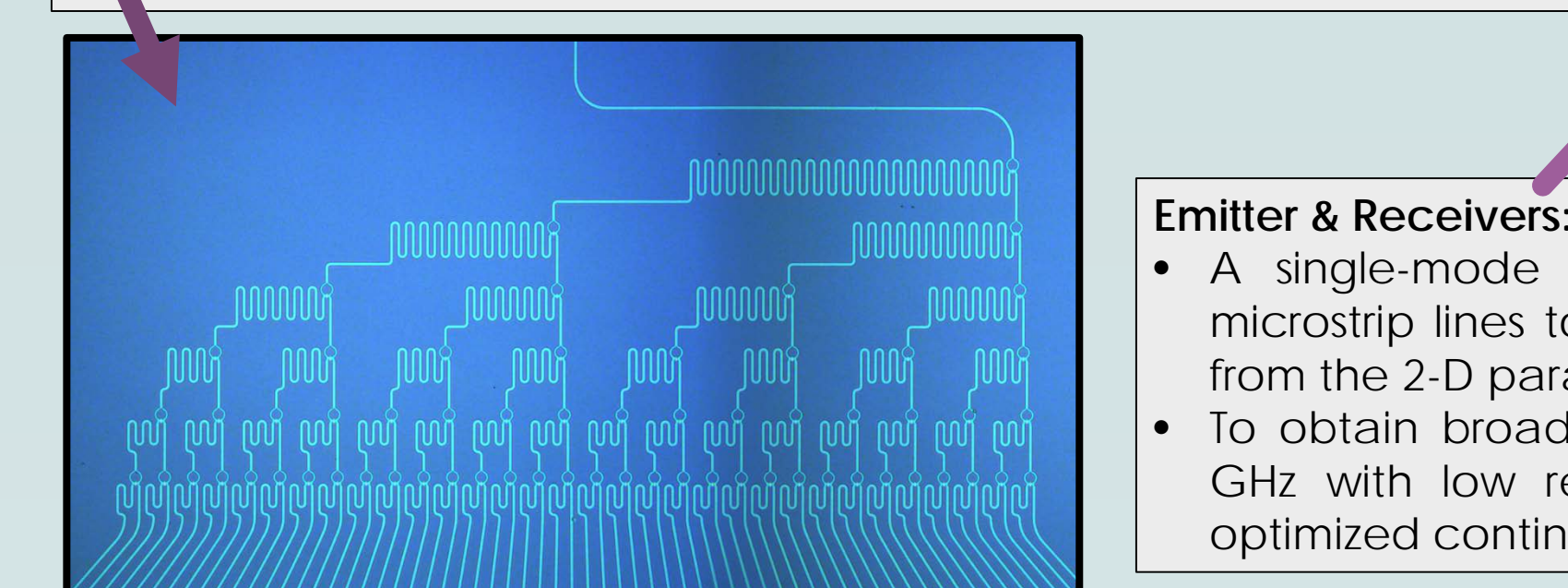
- The slot antenna provides efficient sub-mm-wave coupling from free space over a broad frequency range designed to achieve a 45% fractional bandwidth with return loss better than 12 dB.
- An anti-reflective coated hyper-hemispherical Si lens is used to increase the beam directivity.

'Laboratory' KID Detectors:

- We use Kinetic Inductance Detectors (KIDs) in our implementation because of the simplified readout scheme, their demonstrated low-NEP capability, and their easy integration into our fabrication process.
- We have implemented Al films in the R-64 prototype spectrometer, in a laboratory microstrip transmission line KID design which is well suited for testing with an external sub-mm source with power ~ 1 nW, as well as a cryogenic blackbody source with power ~ 20 pW.

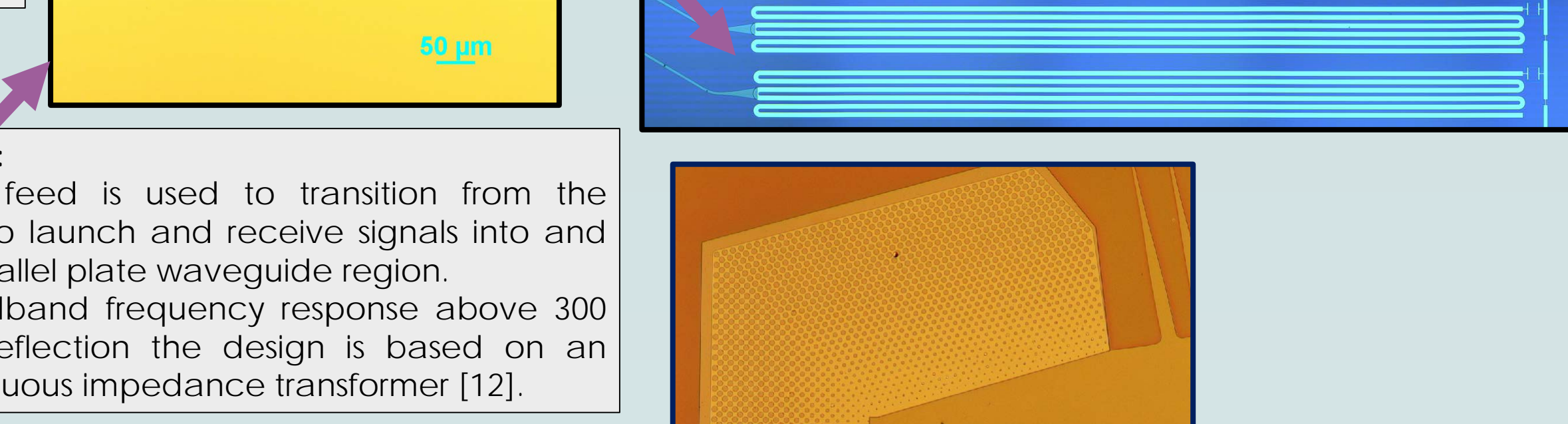
Phase Delay Network:

- The light is split into N equal beams and a linear phase gradient across the pupil is introduced in a network of meandered superconducting Nb microstrip transmission lines.
- The high refractive index of Si allows the large phase delays for an $R=1500$ spectrometer in ≤ 10 mm² area on a Si wafer.
- We use a design algorithm in which the delay lines are broken into multiple sections distributed within a binary power splitter network. This reduces the required area by a factor of $\log_2(N)/(N-1)$.



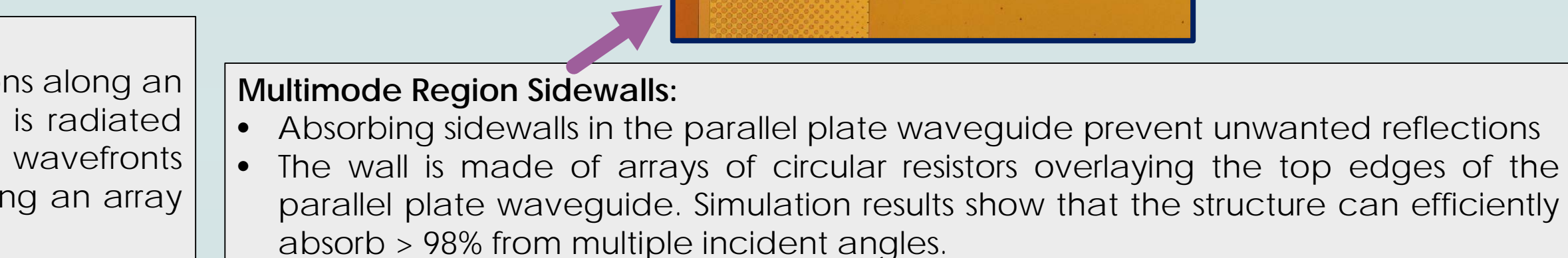
Emitter & Receivers:

- A single-mode feed is used to transition from the microstrip lines to launch and receive signals into and from the 2-D parallel plate waveguide region.
- To obtain broadband frequency response above 300 GHz with low reflection the design is based on an optimized continuous impedance transformer [12].



Focal Plane Design [10]

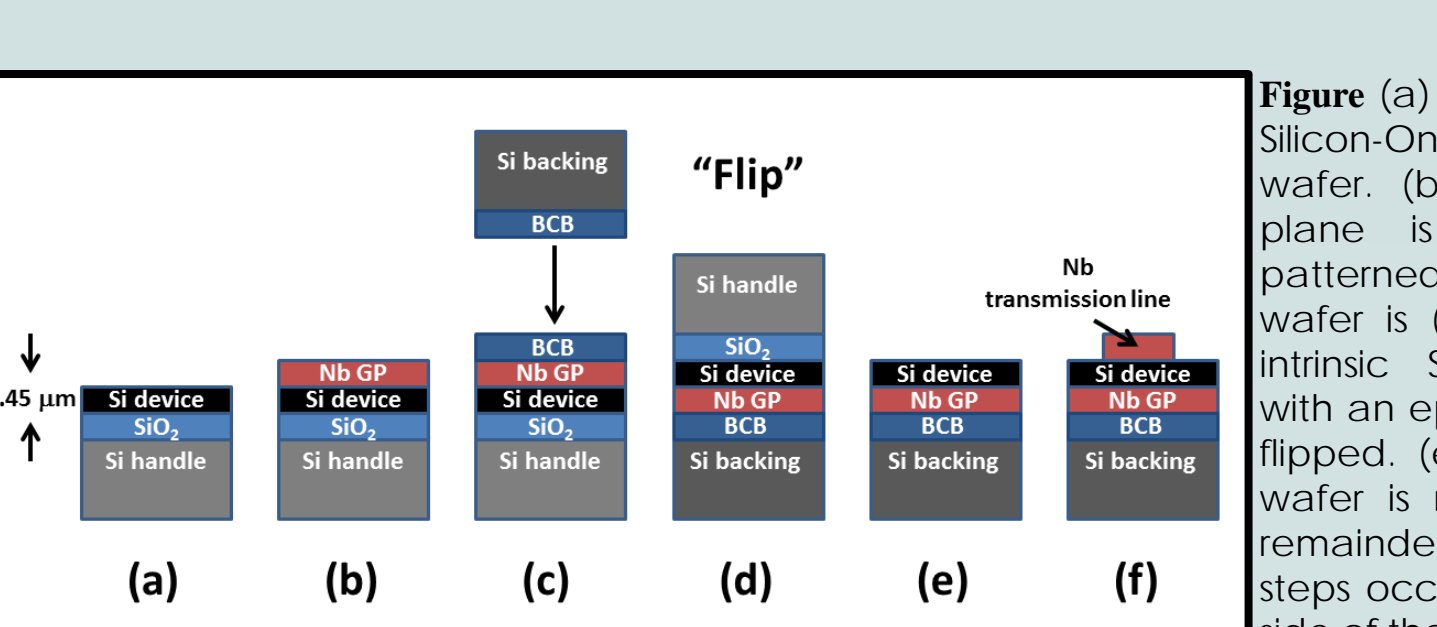
The outputs from the delay network lines are emitted at spaced locations along an approximately circular arc in a Rowland Configuration and the light is radiated into a 2-D parallel plate waveguide region. The convergent circular wavefronts from the different wavelengths of light focus at different locations along an array of receiver feeds at the focal curve.



Multimode Region Sidewalls:

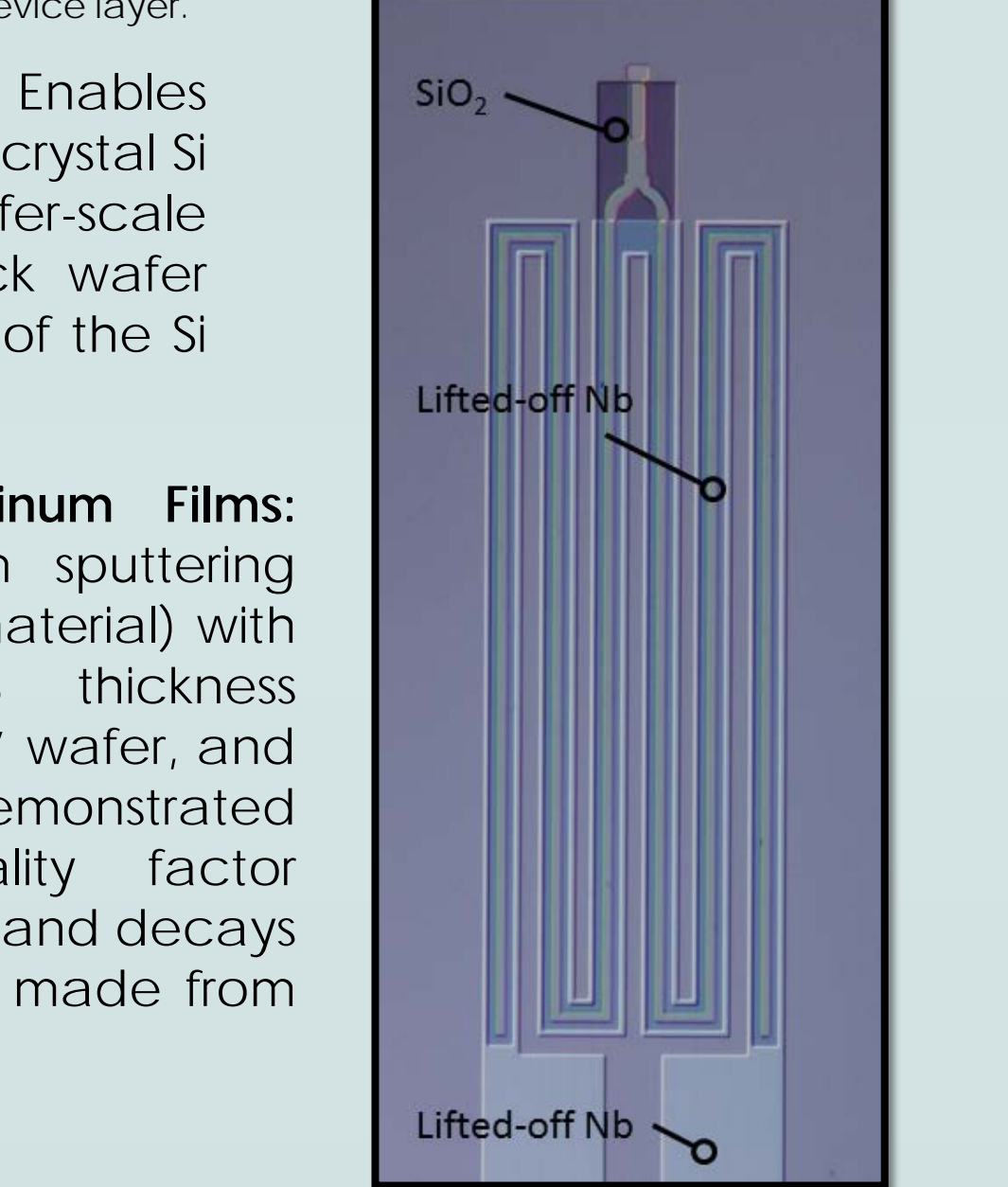
- Absorbing sidewalls in the parallel plate waveguide prevent unwanted reflections.
- The wall is made of arrays of circular resistors overlaying the top edges of the parallel plate waveguide. Simulation results show that the structure can efficiently absorb $> 98\%$ from multiple incident angles.

Fabrication & Materials Milestones:



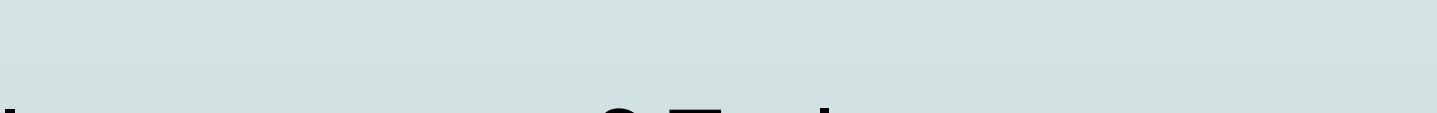
'Single Flip' wafer-scale bonding and thinning process: Enables fabrication of superconducting circuitry on 0.45 μ m single-crystal Si substrate. This is a novel void-free low temperature wafer-scale bonding technique which enables precise front-to-back wafer alignment (within 0.3 μ m) and maintains pristine integrity of the Si dielectric [1].

Nb liftoff process: Enables fabrication of superconducting circuits with better than 0.3 micron linewidth control over a 4" wafer without etching the substrate [2].



High Quality Aluminum Films:

High quality Al film sputtering deposition (for KID material) with better than 0.3% thickness uniformity across a 4" wafer, and quality. We have demonstrated high internal quality factor $0.7 \times 10^6 < Q_i < 2.5 \times 10^6$ and decays times ~ 1 ms in KIDs made from these aluminum films.



Impact of Tolerances:

- We use single-crystal which has a known and very uniform dielectric constant.
- SOITEC SOI wafers have device layers with extremely uniform thickness. The 0.45 μ m thick silicon device layers have measured thickness variations ≤ 4 nm RMS over 1 cm² area, and the Si surface roughness of the finished spectrometers is < 0.5 nm rms. An indication that we have an extremely uniform and well-behaved dielectric material providing good uniformity and design reliability.
- Our studies show that these tolerances will provide the necessary phase control to allow up to $R=2000$ given our measured relevant parameters (Si thickness, Nb transmission line width and resistivity variations).

Materials Development in Progress:

- We achieve yields $> 80\%$ on our devices following our full spectrometer fabrication process and are able to achieve low loss Al and Nb films in single-layer processes.
- We find that the Al and Nb thin films are much more lossy after fabrication of the spectrometers is complete.
- We are investigating the sources of the loss, and initial studies suggest that the loss is related to the presence of dielectric or resistive layers at materials interfaces.

Impact of Loss:

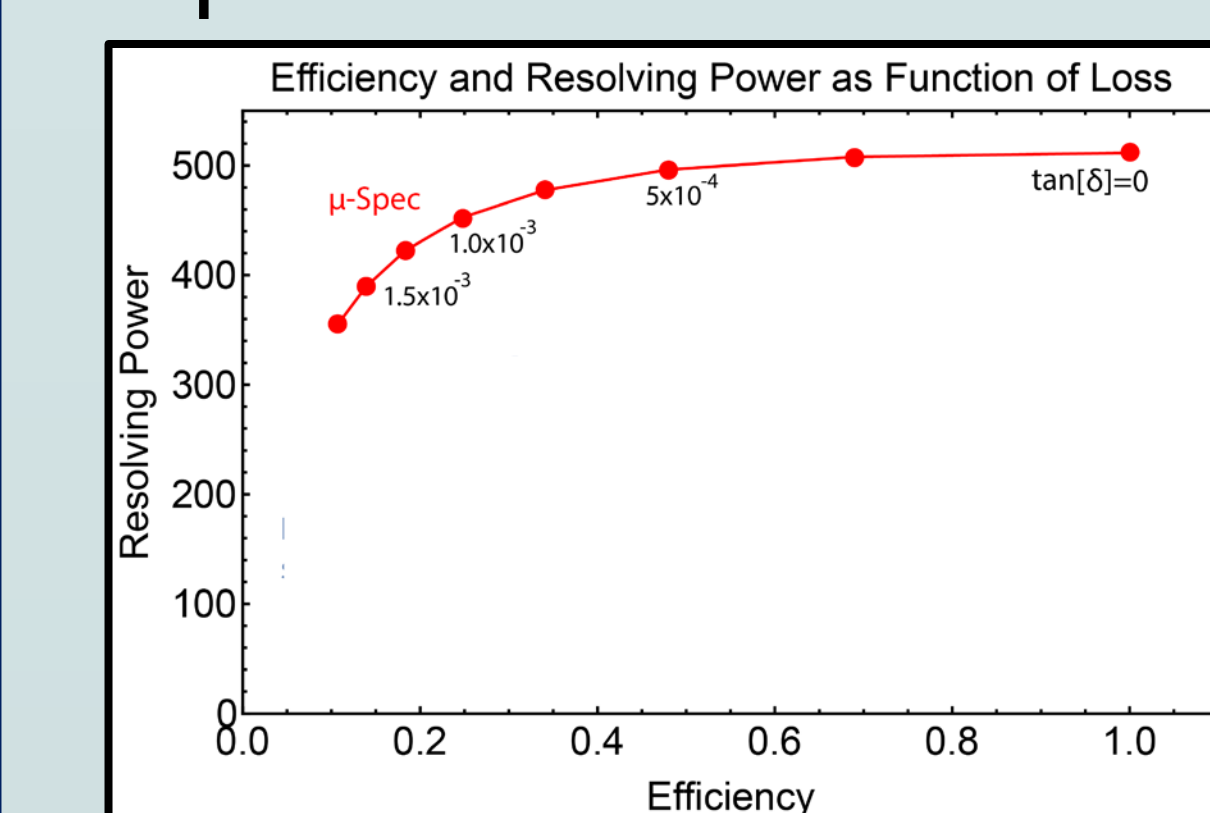


Figure: Efficiency and Resolution as a function of loss for a R=500 μ -Spec.

- The diffraction-grating design of μ -Spec allows it to achieve unity efficiency in principle at its design resolution.
- The ultimate limit to μ -Spec resolution and efficiency is set by the line loss of our material system. We have chosen to implement single-crystal Si which has more than an order of magnitude lower loss than deposited dielectrics (such as Si₃N₄) with $\tan \delta \sim 1 \times 10^{-5}$ [3-6] (and even better when loss reduction processes are applied [7-9]) which should allow up to $R=1500$.
- Additionally, optimization of our design is insensitive to the precise loss value (it does not need to be known a priori).

Stray Light & Cross-talk:

- The integrated optics of our design provide a highly protected environment.
- The use of microstrips for our sub-mm transmission lines and KIDs provides good immunity to stray light, and very low KID-to-KID crosstalk.
- Loss above the superconducting gap prevents unwanted coupling.
- The microwave readout feedlines are protected via thermal blocking filters [13].
- We measure an out-of-band response in our R=64 prototype that is null over the full instrument band (see right) using a 100/Ohms square backside coating.
- We have also measured the response of a dark detector adjacent to an illuminated device. The signal was $< 2.5 \times 10^{-4}$ of the illuminated one, ruling out cross-talk via the KIDs, readout line, substrate, or leakage around the antenna baffling.
- We are considering for future implementations boxing the spectrometer at the detector temperature [14] and using a NbTiN microstrip feedline.

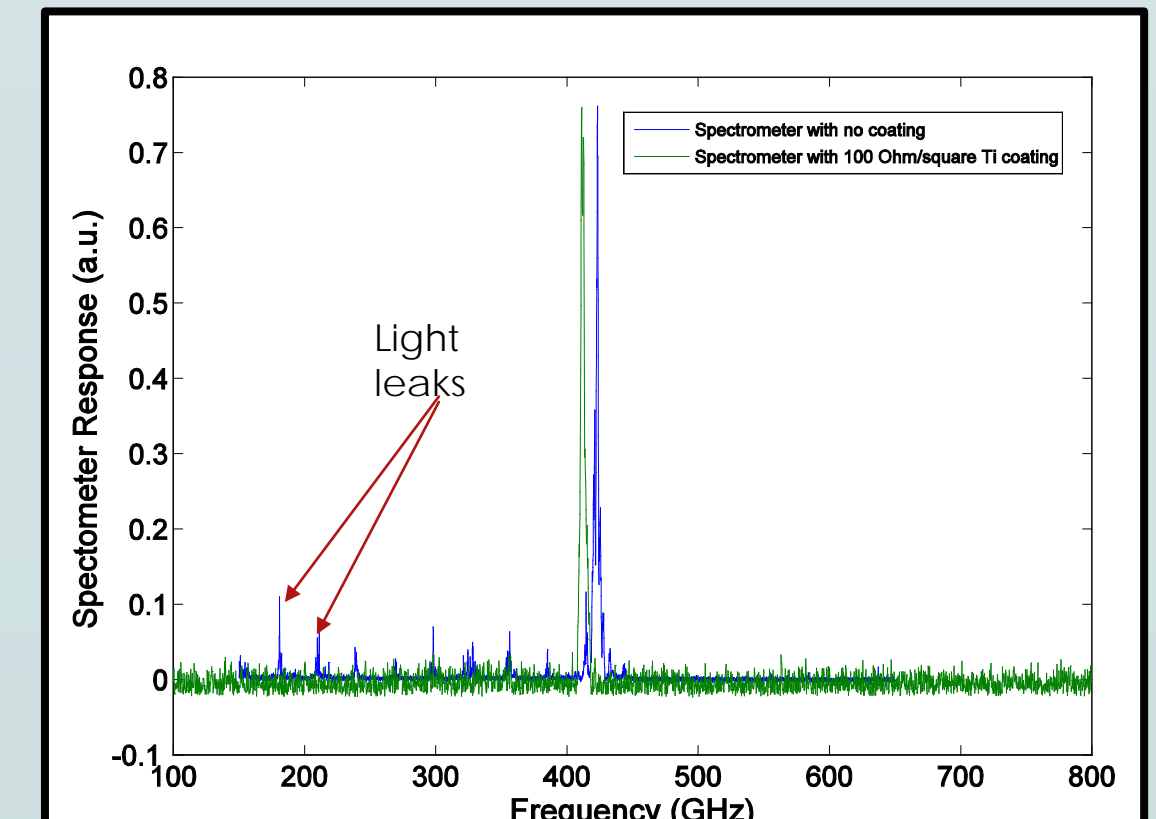
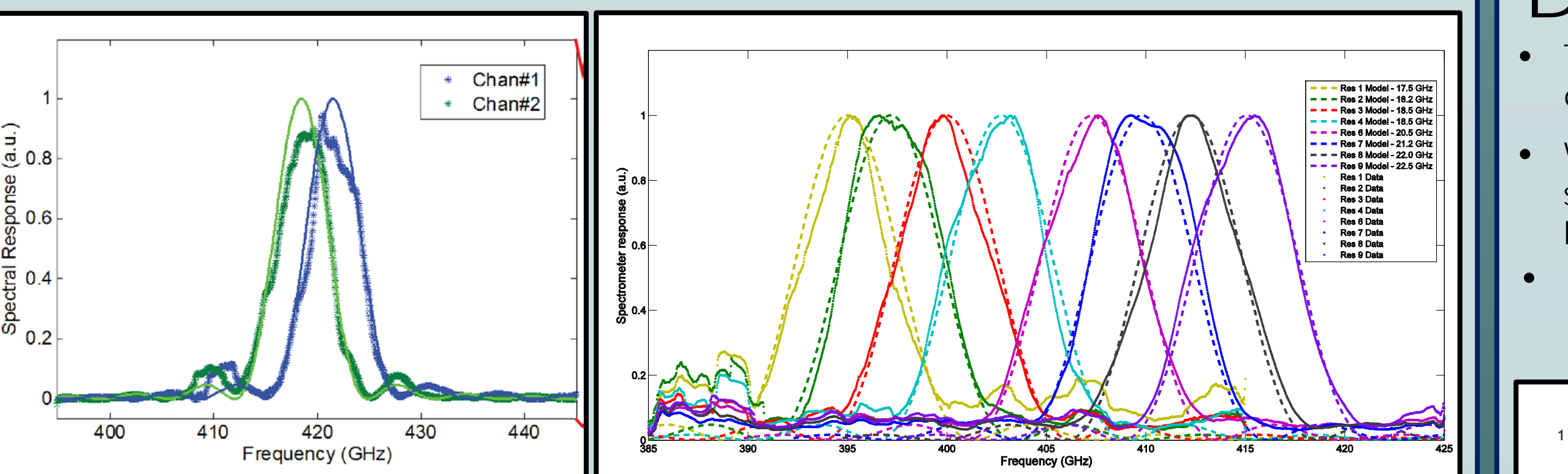


Figure: We are able to eliminate narrow-band harmonic optical responses due to a sub-mm light leak which coupled through the CPW readout line, by depositing a thin Ti absorber (~ 100 Ohms/sq) on the backside of the Si handle wafer to terminate stray radiation.

R=64 Resolution Demonstration:



We have demonstrated the spectrometer's line profile, absolute frequency and resolution to design. For device v.1 (left), we saw absolute frequency response to design within ± 1 GHz source frequency error. For device v.2 (right) a layer with a low superconducting gap in one of our Nb layers shifted the frequencies by 20 GHz from our design target, though the resolution and line profile were retained.

Design of an R=256 & 512 μ -Spec for Balloon-Flight:

- The designs of the R=256 & 512 μ -Spec instruments are derived directly from the R=64 prototype and rely on the use of these demonstrated spectrometer components, with modifications to the focal plane design and KID detector sensitivity requirements.
- We have preliminary designs for the R=256 and R=512 focal planes [11]. These designs run in higher orders with high ($\sim 80-90\%$) efficiency, assuming Nyquist sampling of the focal plane. In this implementation each receiver will receive an optical signal across three to five orders in optical frequency (see Table). Broadband order-sorting filters will be inserted at the output of each receiver to separate these orders, before each is sent to a KID detector.
- The size of the parallel plate waveguide region is set only by the required number of emitters and receivers. When scaling to higher resolving powers, the multimode region size need not increase. As we scale toward $R=1500$ we expect the instrument size to be dominated by the area of the detectors.

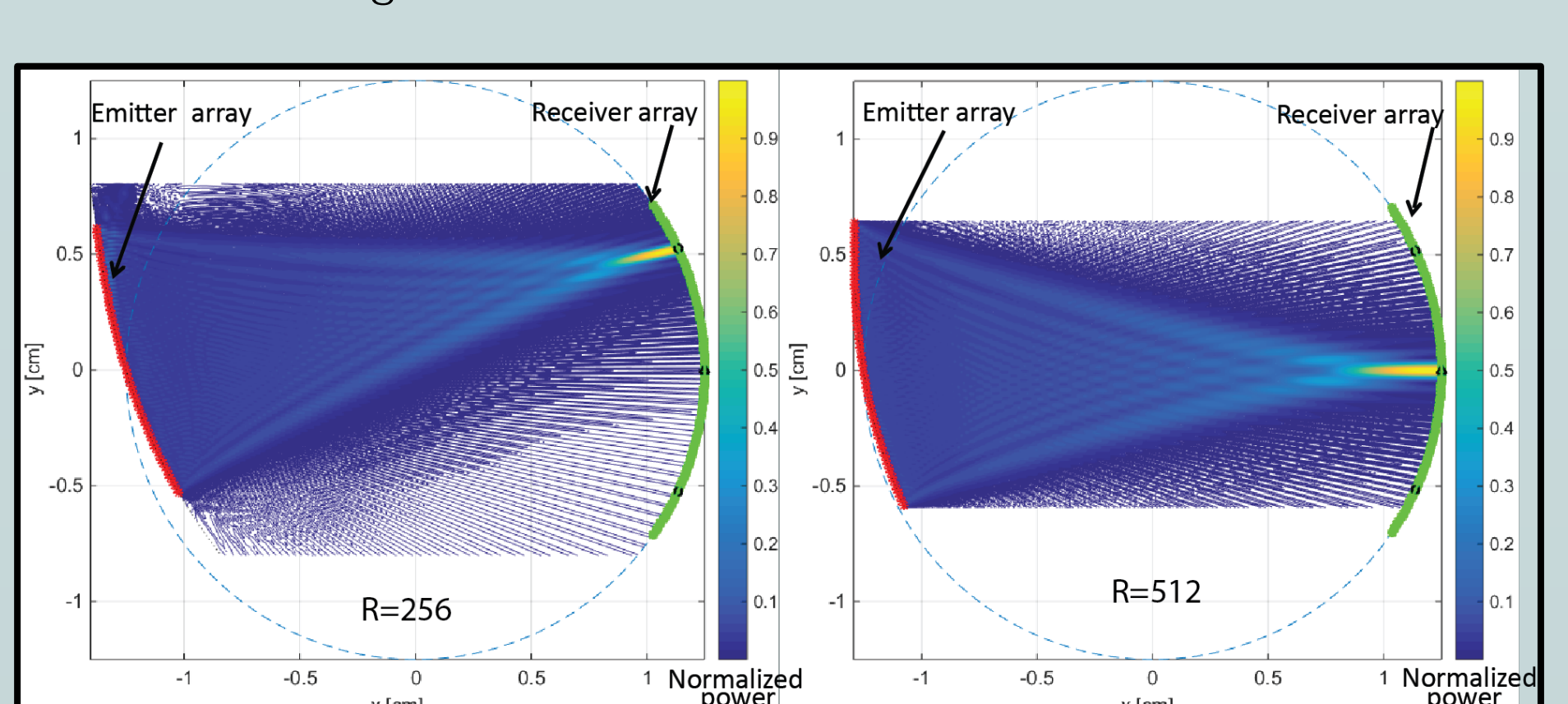


Figure: Left: Preliminary R=256 design, showing power distribution at 430 GHz in the lower end of the 3rd order. RMS phase error on the focal plane is < 0.005 rad over the full spectral range. Right: Preliminary R=512 design, showing power distribution at 313 GHz at the center of the 4th order. RMS phase error on the focal plane is < 0.015 rad over the full spectral range.

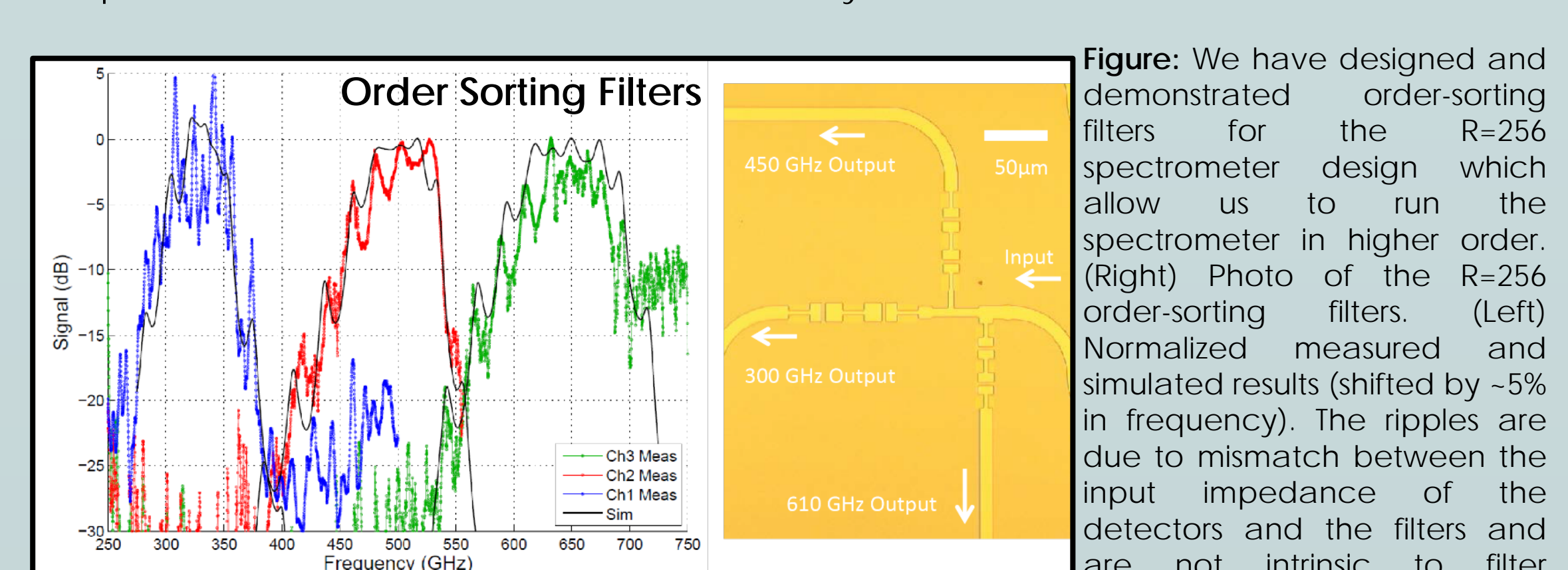


Figure: We have designed and demonstrated order-sorting filters for the R=256 spectrometer design which allow us to run the spectrometer in higher order. (Right) Photo of the R=256 order-sorting filters. (Left) Normalized measured and simulated results (shifted by $\sim 5\%$ in frequency). The ripples are due to mismatch between the input impedance of the detectors and the filters and are not intrinsic to filter performance.

References

- A. Patel et al., IEEE Trans. on Appl. Supercond., 2013.
- Brown, A., Patel, A., High Precision Metal Liftoff Technique, U.S. Patent No. 9,076,658 B1, 2015.
- R. Datta et al., "Large-aperture wide-bandwidth antireflective-coated silicon lenses for millimeter wavelengths," Applied Optics, vol. 52, no. 36, pp. 8747-8758, 2014.
- T. Duffar, Crystal Growth Processes Based on Capillarity, Czochralski, Floating Zone, Shaping and Crucible Techniques, Wiley, 2010.
- J. Krupka et al., "Measurements of permittivity, dielectric loss tangent, and resistivity of float-zone silicon at microwave frequencies," IEEE Transactions on Microwave Theory and Techniques, vol. 54, pp. 3995-4000, 2006.
- M. N. Asfar and H. Chi, "Millimeter wave complex refractive index, complex dielectric constant, and loss tangent of extra high purity and compensated silicon," International Journal of Infrared and Millimeter Waves, vol. 15, pp. 1181-1188, 1994.
- M. N. Asfar and H. Chi, "Window Materials for High Power Gyrotron," International Journal of Infrared and Millimeter Waves, vol. 15, no. 7, pp. 1161-1179, 1994.
- V. V. Parshin et al., "Silicon as an Advanced Window Material for High Power Gyrotrons," International Journal of Infrared and Millimeter Waves, vol. 16, pp. 863-877, 1995.
- J. Mollá et al., "Radiation Effects on Dielectric Losses of Au-Doped Silicon," Journal of Nuclear Materials, 258-263, pp. 1883-1888, 1998.
- G. Cataldo et al., "Micro-Spec: an ultra-compact high-sensitivity spectrometer for far-infrared and submillimeter astronomy," Applied Optics, vol. 53, no. 6, pp. 1094-1102, 2014.
- G. Cataldo et al., "Micro-Spec: an integrated direct-detection spectrometer for far-infrared space telescopes," In Space Telescopes and Instrumentation 2014: Optical, Infrared, and Millimeter Wave, vol. 9143 of Proceedings of SPIE, pp. 91432C1-9, 2014.
- Pietini, D., Popescu, C. C., Tufts, R. J., & Volk, H. "Astronomische Nachrichten Supplement, 324, 164, 2003.
- Wollack, E. J. et al. "Impedance Matched Absorptive Thermal Blocking Filters," Review of Scientific Instruments, in press, Vol. 85, No. 3; <http://arxiv.org/abs/1403.2909>, 2014.
- Crowe, E. J. et al. "Fabrication of a Silicon Backshort Assembly for Waveguide-Coupled Superconducting Detectors," IEEE Transactions on Applied Superconductivity, vol. 23, no. 3, p. 2500505, 2013.

Table: Specifics of a preliminary R=256 & R=512 designs which we hope to implement.

Resolving power R	Radius (cm)	Chip size (cm ²)	# of emitters	# of receivers	# of detectors	Receiver spacing (mm)	Order in use	Bandwidth (GHz)	Average efficiency
256	1.25	$\sim 4 \times 3$	64	237	949	165	2 to 4	300-650	88%
512	1.25	$\sim 4 \times 3$	64	241	1205	163	4 to 8	303-650	88%

Table: KID design requirements for balloon-flight, assuming measured properties of our Al films.

	Current "Laboratory"	Proposed R=256 (Warm Balloon)	Proposed R=512 (Cold Balloon)
Optical freq.	~ 500 GHz	~ 500 GHz	~ 500 GHz
Optical Loading	1nW-20 pW	30 fW	50 aW
Power	1nW-20 pW	30 fW	50 aW
HEMT Noise Temp.	5 K	5 K	5 K
Al width	17.3 μ m	3.2 μ m	3.2 μ m
Al thickness	100 nm	20 nm	20 nm
Al total length	~ 15.2 mm	~ 6.8 mm	~ 6.8 mm
Q _i under loading	20,000 - 137,000	300,000	800,000
Readout freq.	2.1 - 2.5 GHz	2.8 - 3.0 GHz	2.8 - 3.0 GHz
Detector NEP	$1.5 \times 10^{-15} - 5.5 \times 10^{-17}$ W/Hz ^{1/2}	8×10^{-18} W/Hz ^{1/2}	3.5×10^{-18} W/Hz ^{1/2}
BLIP NEP	$9 \times 10^{-18} - 4 \times 10^{-19}$ W/Hz ^{1/2}	5×10^{-19} W/Hz ^{1/2}	2×10^{-19} W/Hz ^{1/2}